

1 **Supplementary Fig. 1**

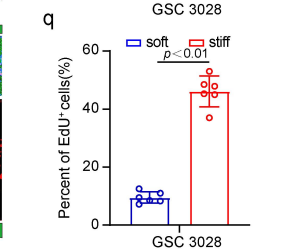
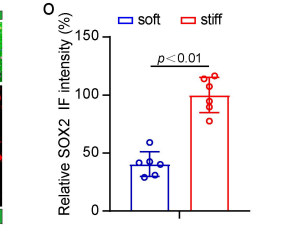
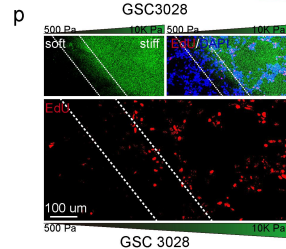
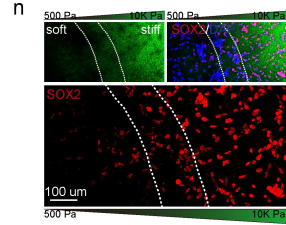
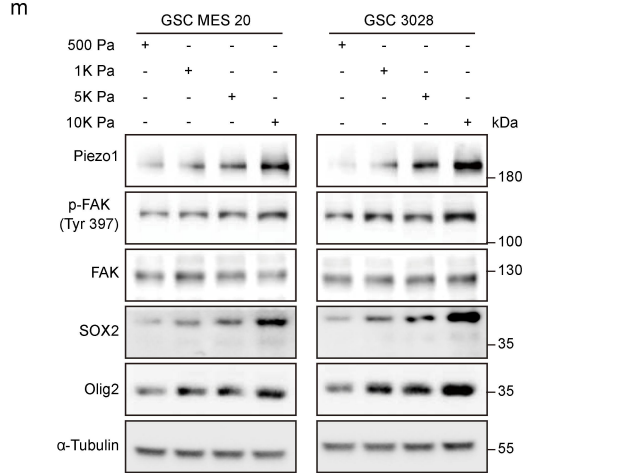
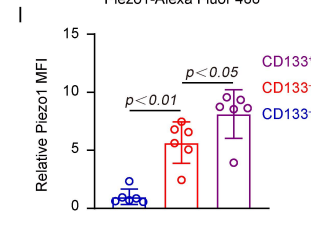
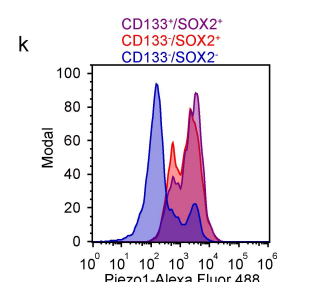
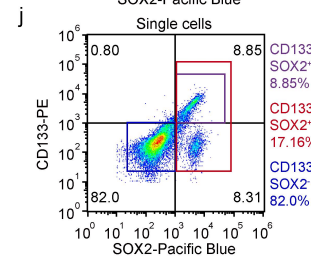
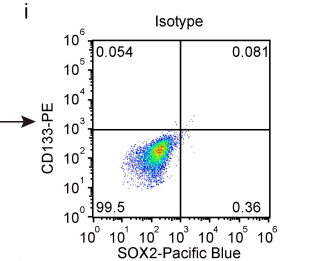
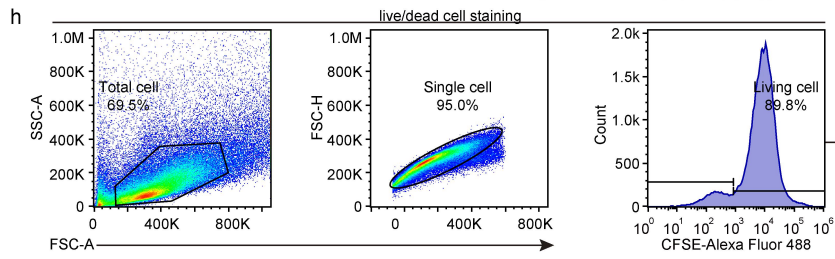
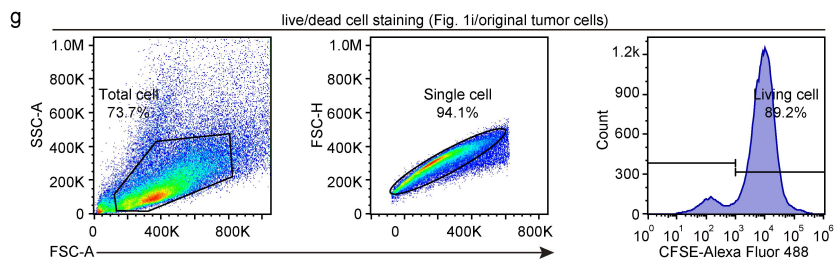
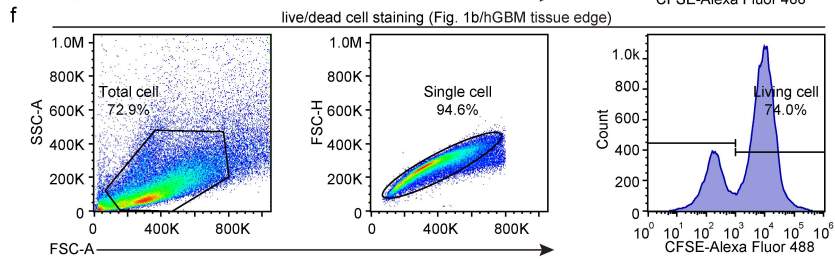
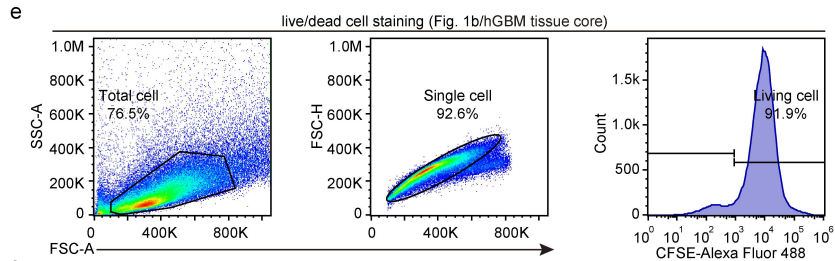
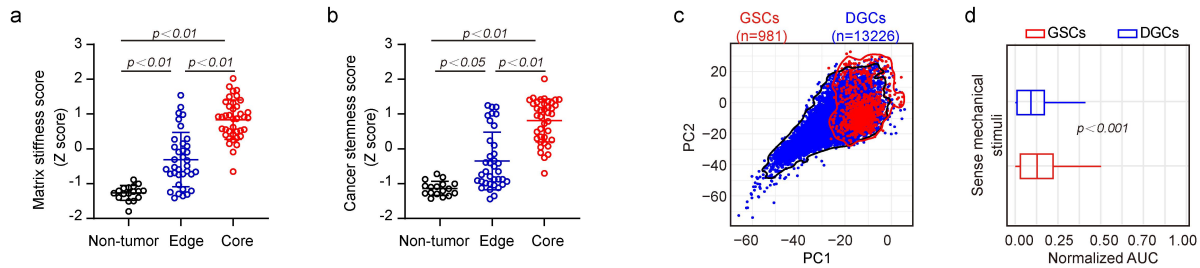
2 **a**, MES20 glioblastoma stem cells (GSCs) were transduced with either a non-targeting control shRNA (shCONT)
 3 or increasing concentrations of an shRNA targeting Piezo1 (shPiezo1). mRNA was collected, and Piezo1 gene
 4 expression relative to GAPDH levels was measured by qPCR.

5 **b, c**, Knockdown efficiencies of PIEZO1 in GSC MES20 are displayed, Cellular lysates for cells from (a) were
 6 collected and resolved by SDS-PAGE. Western blot analysis (**b**) and quantitative analysis (**c**) of GSCs (MES20)
 7 after PIEZO1 knockdown.

8 **d, e**, Immunofluorescence staining (**d**) and quantitative analysis (**e**, $n = 6$ randomly selected fields per group)
 9 of GSCs (MES20) following knockdown of PIEZO1 at different levels.

10 In **a, c** and **e**, data are presented as mean \pm s.d. In **b** immunoblots are representative of three independent
 11 experiments with similar results. In **a, c** and **e** data are presented from three independent experiments.

12 One-way ANOVA followed by multiple comparisons for **a, c** and **e**.



13 **Supplementary Fig. 2**

14 **a, b**, Sequencing data from different regions of GBM samples were analyzed (GSE59612), and the matrix
15 stiffness score (**a**) and stemness score (**b**) were quantified for the non-tumor (n = 17), tumor edge (n = 36),
16 and tumor core (n = 39) regions.

17 **c, d**, Quantification of the ability to sense mechanical stimulation in scRNA-seq data from 14,207 malignant
18 cells of seven GBM patients.

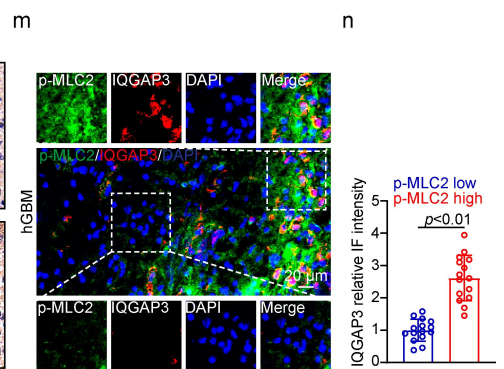
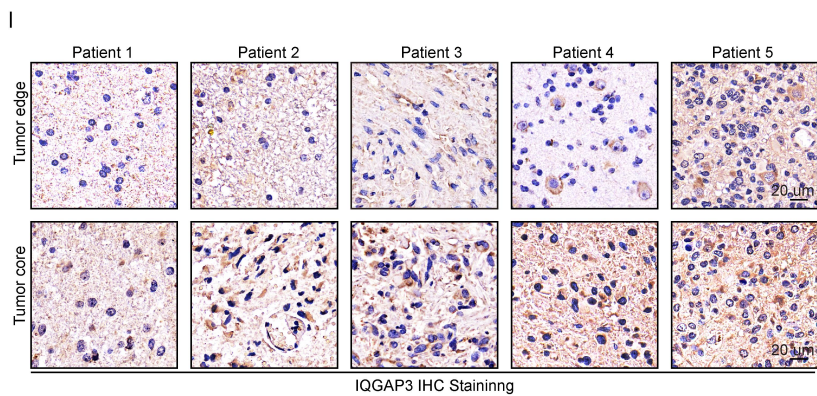
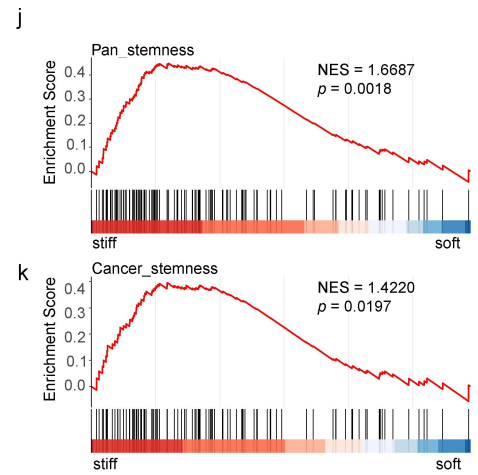
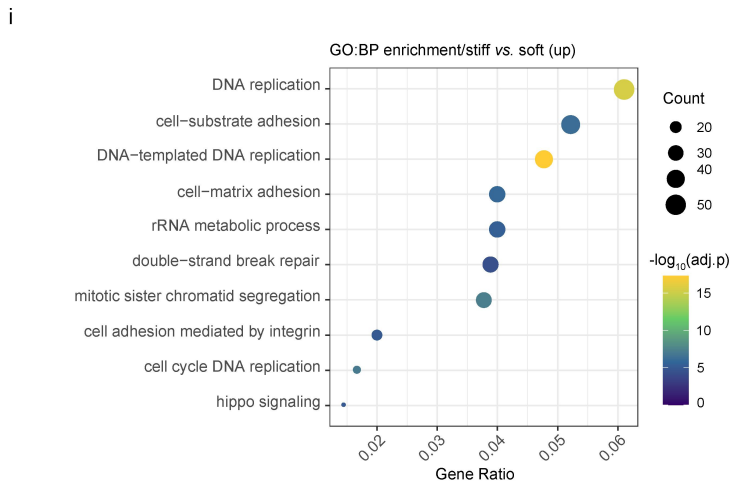
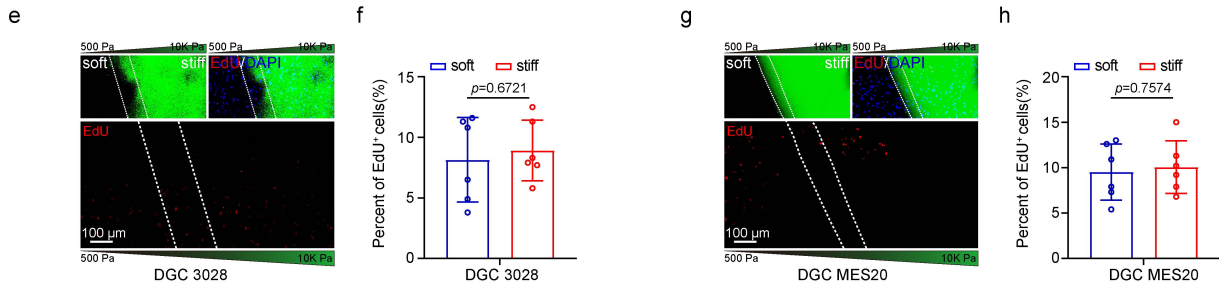
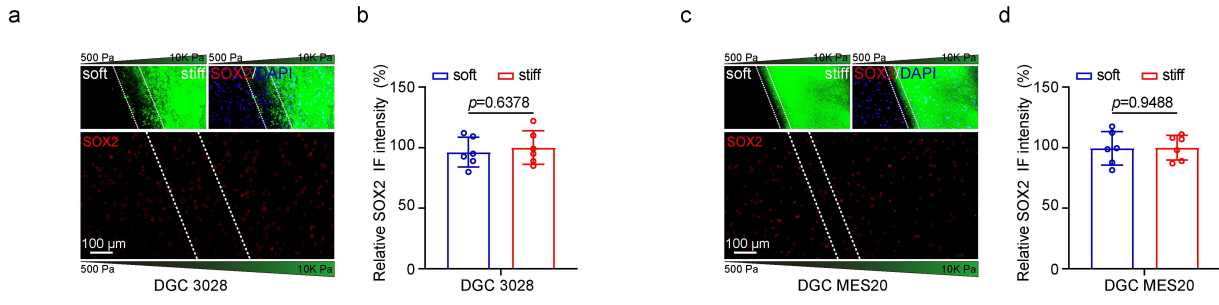
19 **e - h**, Live/dead cell staining analysis by flow cytometry.

20 **i - l**, Gating strategy (**i** and **j**), representative histogram plots (**k**), and statistical quantification **l**, n = 6 GBM
21 samples per group) of Piezo1 flow cytometric analysis for the indicated cell populations in GBM samples. MFI,
22 median fluorescence intensity.

23 **m**, Immunoblot of GSCs cultured on matrices with different stiffness levels.

24 **n - q**, GSC 3028 cultured on diffusion-based polyacrylamide stiffness gradient gels were subjected to
25 immunofluorescence staining (**n**) and statistical quantification (**o**, n = 6 randomly selected fields per group) as
26 well as quantification of EdU incorporation (**p** and **q**, n = 6 randomly selected fields per group). Stronger
27 green fluorescence indicates higher matrix stiffness. IF: Immunofluorescence.

28 In **a, b, l, o** and **q**, data are presented as mean \pm s.d. In **m** immunoblots are representative of three
29 independent experiments with similar results. In **o** and **q**, data are presented from three independent
30 experiments. Two-tailed paired t-test for **o** and **q**. One-way ANOVA followed by multiple comparisons for **a, b**
31 and **l**.



32 **Supplementary Fig. 3**

33 **a - h**, DGCs (3028 and MES20) cultured on diffusion-based polyacrylamide stiffness gradient gels were
34 subjected to immunofluorescence staining (**a** and **c**) and statistical quantification (**b** and **d**, $n = 6$ randomly
35 selected fields per group) as well as quantification of EdU incorporation (**e - h**, $n = 6$ randomly selected fields
36 per group). Stronger green fluorescence indicates higher matrix stiffness.

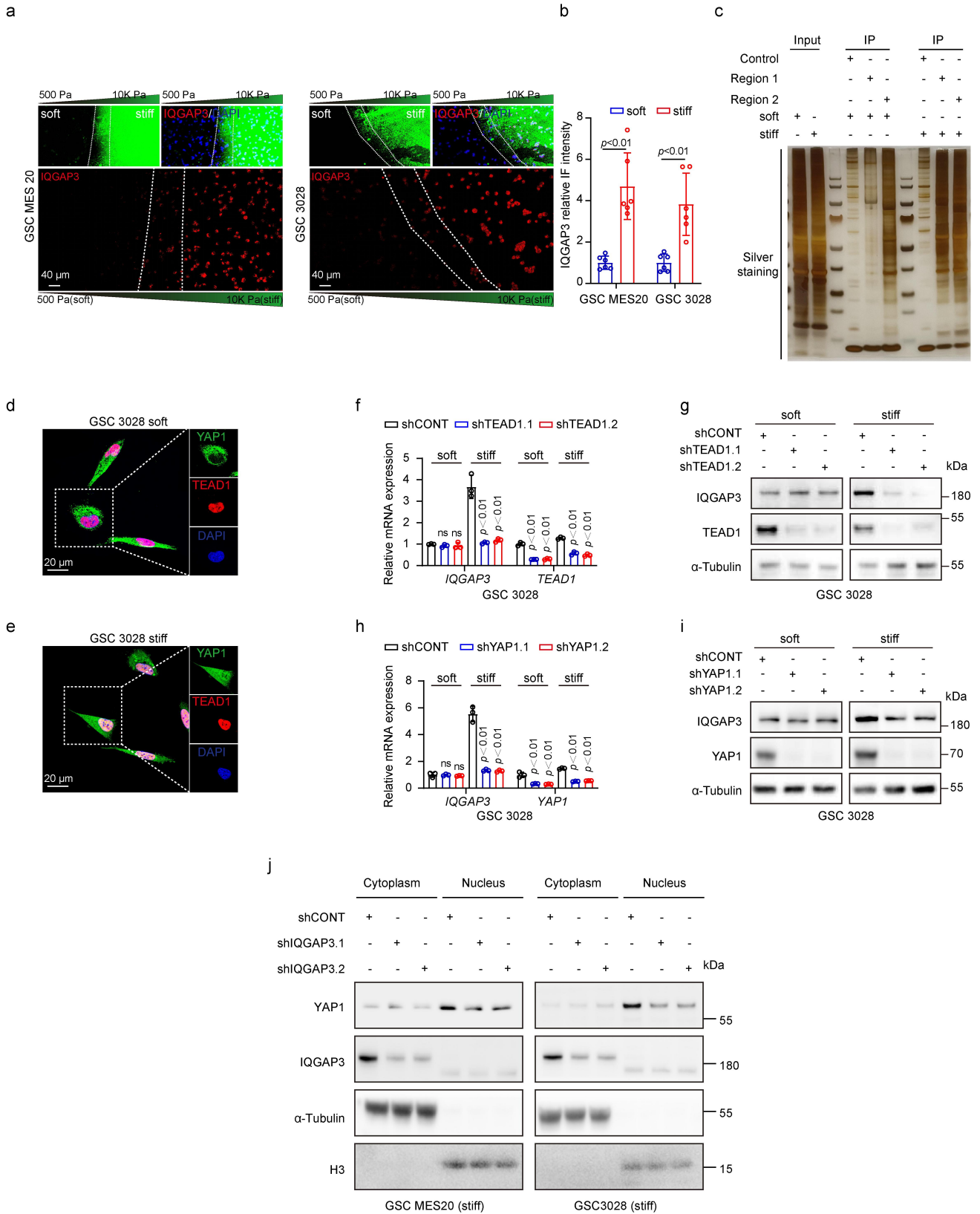
37 **i**, GO enrichment analysis of biological processes (GOBP) for genes upregulated in GSCs (stiff) compared to
38 GSCs (soft).

39 **j, k**, GSEA analysis of GOBP. NES, normalized enrichment score.

40 **l**, Immunohistochemical staining shows the expression of IQGAP3 protein in different regions of GBM.

41 **m, n**, Immunofluorescence staining (**m**) and quantitative analysis (**n**, $n = 15$ randomly selected fields
42 examined over 5 GBM sample per group) of GBM tissue sections. IF: Immunofluorescence

43 In **b, d, f, h** and **n**, data are presented as mean \pm s.d. In **b, d, f** and **h**, data are presented from three
44 independent experiments. Two-tailed unpaired t-test for **b, d, f, h** and **n**. Weighted Kolmogorov–Smirnov
45 statistic test for **j** and **k**. In **i - k**, transcriptomic data are from three biologically independent samples per
46 group. IF: Immunofluorescence.



47 **Supplementary Fig. 4**

48 **a, b**, GSCs (MES20 and 3028) cultured on diffusion-based polyacrylamide stiffness gradient gels were
49 subjected to immunofluorescence staining (a) and statistical quantification (b, n = 6 randomly selected fields
50 per group). Stronger green fluorescence indicates higher matrix stiffness.

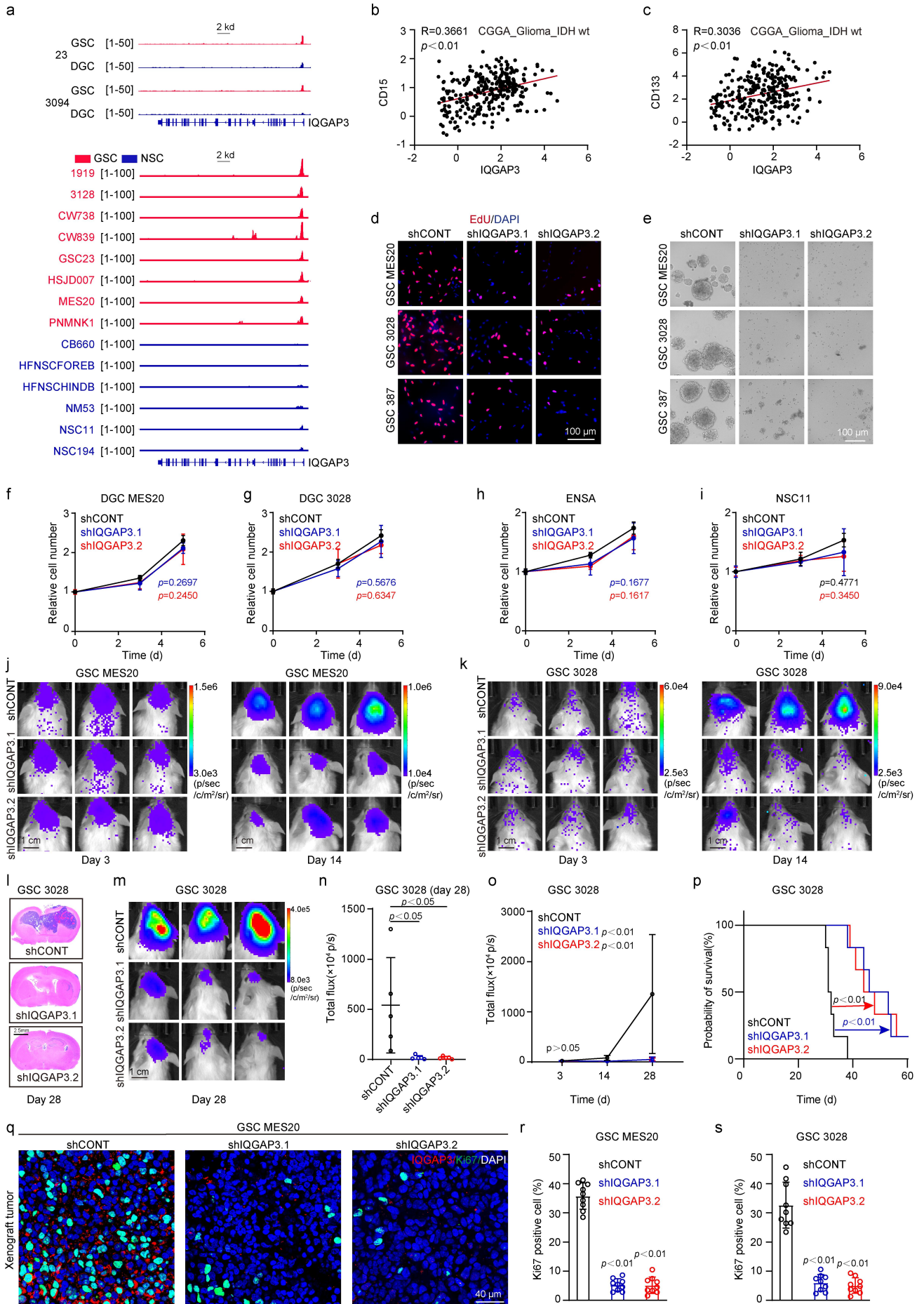
51 **c**, Silver staining shows protein binding to the IQGAP3 promoter region in GSCs cultured on substrates with
52 different stiffness.

53 **d, e**, Immunofluorescence shows the nuclear localization of YAP1 protein and the expression of IQGAP3
54 protein in GSCs (3028) cultured on soft substrate (**d**) and stiff substrate (**e**).

55 **f - i**, RT-qPCR (**f** and **h**) and immunoblots (**g** and **i**) show that YAP1 and TEAD1 regulate the expression of
56 IQGAP3 protein only in GSC (3028) cultured on stiff substrates.

57 **j**, GSCs (MES20 and 3028) were transduced with either a non-targeting control shRNA sequence (shCONT) or
58 one of two shRNAs targeting IQGAP3 (designated shIQGAP3.1 or shIQGAP3.2), then cultured the cells of stiff
59 matrices. Cytoplasmic and nuclear lysates were collected and resolved by SDS-PAGE. Western blot analysis
60 showed the changes in YAP1 following IQGAP3 knockdown in GSCs cultured on stiff matrix gels.

61 In **b, f** and **h**, data are presented as mean \pm s.d. In **g, i** and **j**, immunoblots are representative of three
62 independent experiments with similar results. In **b, f** and **h**, data are presented from three independent
63 experiments. Two-way ANOVA followed by multiple comparisons for **b, f** and **h**.



64 **Supplementary Fig. 5**

65 **a**, ChIP-seq analysis of H3K27ac signal on IQGAP3 promoter in indicated cells.

66 **b, c**, Pearson correlations between IQGAP3 and CD15 (**b**), CD133 (**c**), were analyzed using RNA-seq data from
67 the CGGA dataset (primary, glioma_IDH_wt, n = 282 patients). Red lines indicate linear regression. IDH_wt:
68 IDH wild type.

69 **d, e**, Representative images of EdU incorporation assay (**d**) and sphere formation assay (**e**) in GSCs (MES20,
70 3028 and 387) with or without IQGAP3 knockdown.

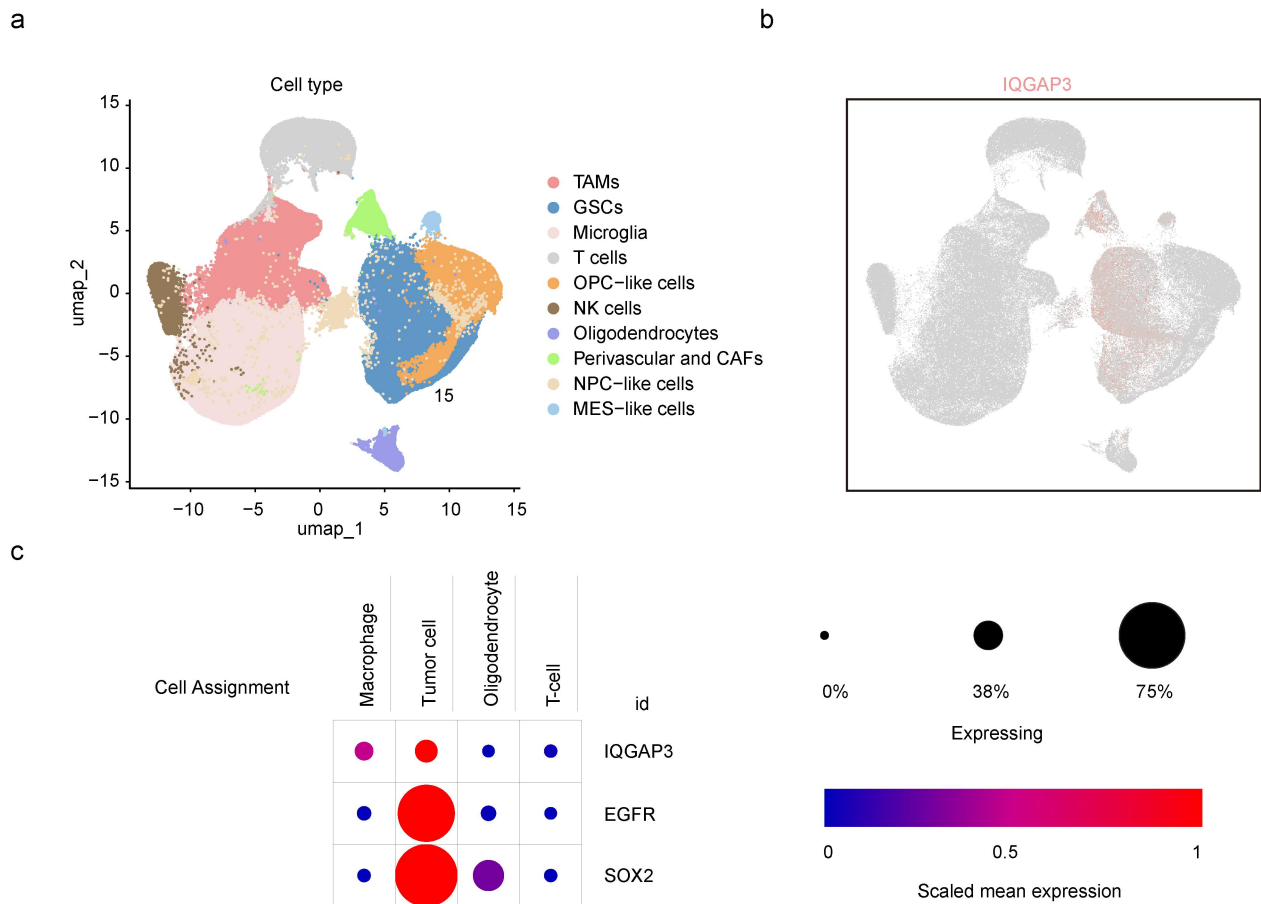
71 **f - i**, Cell viability in DGCs (**f** and **g**) and NSCs (**h** and **i**) with or without IQGAP3 knockdown. (n = 4)

72 **j, k**, Representative in vivo bioluminescence imaging at the indicated timepoints of mice bearing the
73 indicated xenografts.

74 **l - p**, Representative images of hematoxylin and eosin (H&E)-stained brain sections at the indicated timepoint
75 (**l**). Representative in vivo bioluminescence imaging (**m**) and quantification (**n**) at the indicated timepoint of
76 mice bearing the specified xenografts (n = 5 mice per group). Tumor growth curve from in vivo
77 bioluminescence analysis of mice bearing the indicated xenografts (**o**, n = 5 mice per group). Kaplan - Meier
78 survival curves of mice bearing the indicated xenografts (**p**, n = 6 mice per group).

79 **q - s**, Representative images (**q**) and quantifications (**r** and **s**, n = 9 randomly selected fields examined across 3
80 mice per group) of Ki67 (green) and IQGAP3 (red) in brain sections derived from the indicated xenografts.
81 DAPI (blue) was used to stain the nuclei.

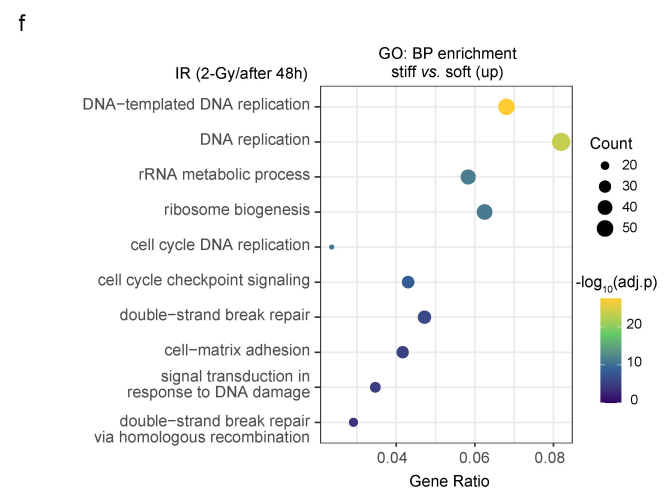
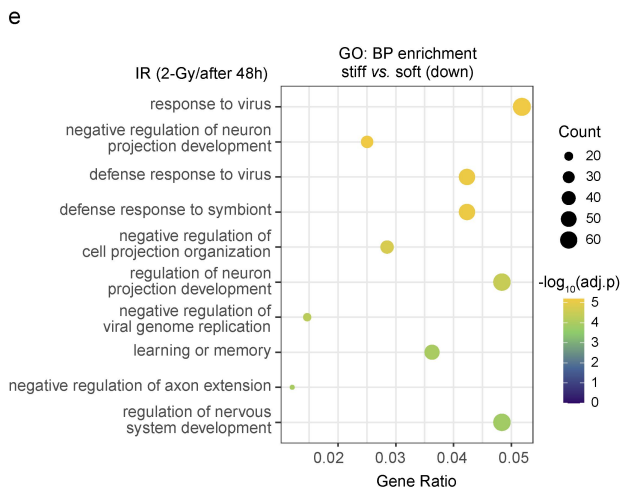
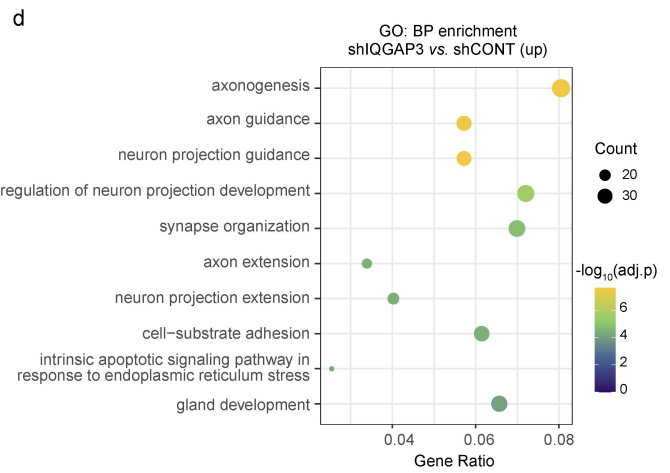
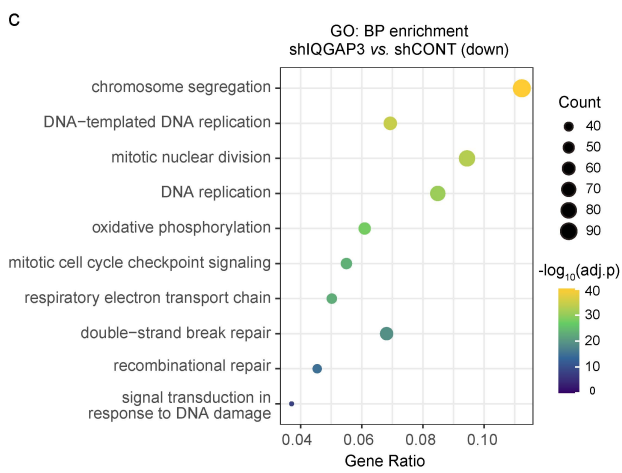
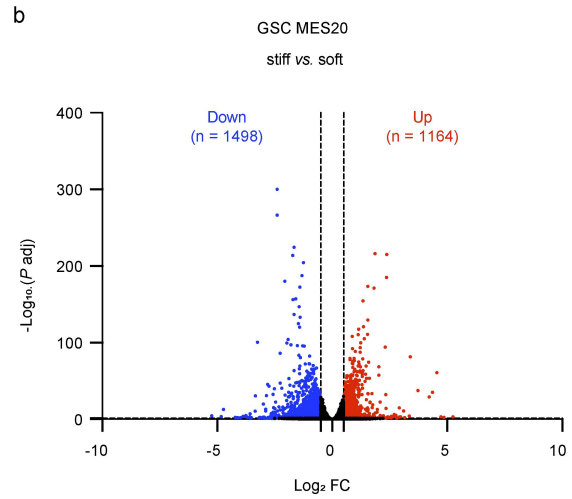
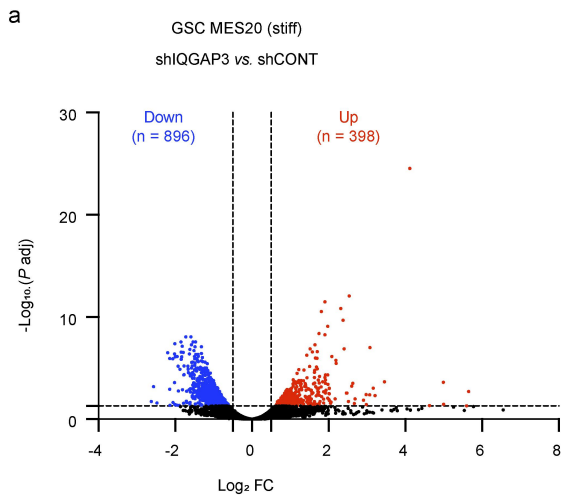
82 In **f - i**, **n**, **o**, **r** and **s**, data are presented as mean \pm s.d. One-way ANOVA followed by multiple comparisons for
83 **n**, **r** and **s**. Two-way ANOVA followed by multiple comparisons for **f - i** and **o**. Two-tailed Pearson correlation
84 for **b** and **c**. Log-rank test for **p**.



85 **Supplementary Fig. 6**

86 **a, b**, Single-cell analysis of glioblastoma (GSE182109) revealed that IQGAP3 was predominantly expressed in
 87 tumor cells.

88 **c**, Single-cell analysis (GSE131928) revealed that IQGAP3, EGFR, and SOX2 were all highly expressed in tumor
 89 cells.



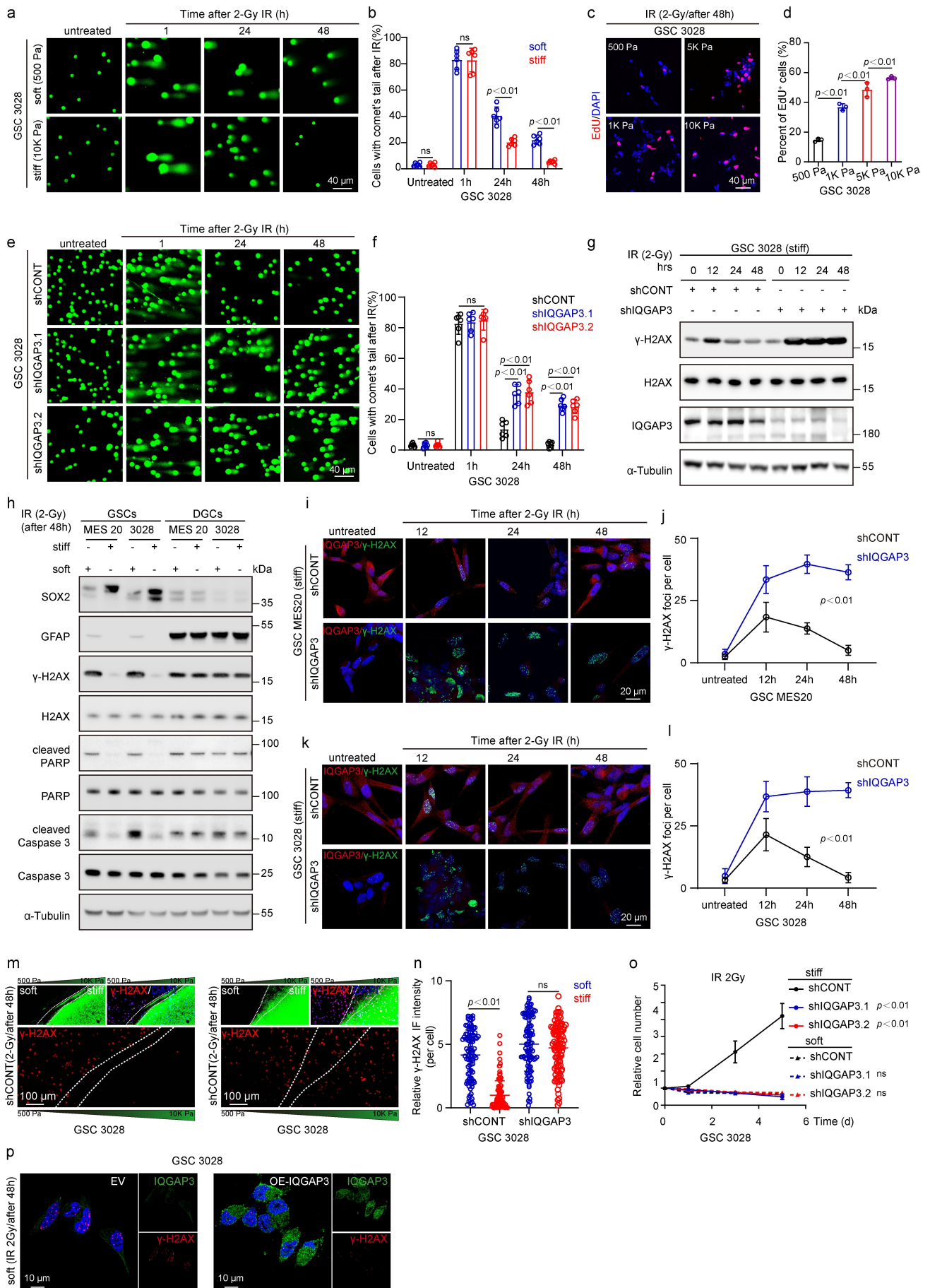
90 **Supplementary Fig. 7**

91 **a**, Volcano plot showing differentially expressed genes (cutoff, $|\log_2(\text{fold change (FC)})| > 0.585$ false discovery
92 rate (FDR) < 0.05) in RNA-seq data of GSCs (shIQGAP3) vs. GSCs (shCONT). Red dots indicate upregulation,
93 and blue dots indicate downregulation in GSCs (shIQGAP3).

94 **b**, Volcano plot showing differentially expressed genes (cutoff, $|\log_2(\text{fold change (FC)})| > 0.585$ false discovery
95 rate (FDR) < 0.05) in RNA-seq data of GSCs (stiff) vs. GSCs (soft) after irradiation. Red dots indicate
96 upregulation, and blue dots indicate downregulation in GSCs (stiff).

97 **c, d**, GO enrichment analysis of biological processes (GOBP) for genes that are downregulated (c) and
98 upregulated (d) in shIQGAP3 compared to shCONT in GSCs (MES20). shCONT: short hairpin (sh) Control.

99 **e, f**, GO enrichment analysis of biological processes (GOBP) for genes that are downregulated (c) and
100 upregulated (d) in GSCs (stiff) compared to GSCs (soft) after irradiation. IR: Ionizing Radiation (X-ray).



101 **Supplementary Fig. 8**

102 **a**, GSC 3028 (soft) and GSC 3028 (stiff) cells were irradiated with 2 Gy of IR. DNA damage at sequential time
103 points post-irradiation was assessed using a single-cell gel electrophoresis assay under alkaline conditions
104 (alkaline comet assay).

105 **b**, Quantification of the percentages of cells with comet tails at different time points after IR in GSC 3028
106 (soft) and GSC 3028 (stiff) populations. (n = 6 randomly selected fields per group)

107 **c, d**, GSC 3028 cells were irradiated with 2 Gy of IR. Representative images of the EdU incorporation assay (**c**)
108 and statistical quantification (**d**) under different matrix stiffness conditions. (n = 3 randomly selected fields
109 per group)

110 **e**, GSC 3028 (stiff) cells, with or without IQGAP3 knockdown, were irradiated with 2 Gy of IR. DNA damage at
111 sequential time points post-irradiation was assessed using a single-cell gel electrophoresis assay under
112 alkaline conditions (alkaline comet assay).

113 **f**, Quantification of the percentages of cells with comet tails at different time points after IR in GSC 3028 (stiff)
114 populations, with or without IQGAP3 knockdown. (n = 6 randomly selected fields per group).

115 **g**, Immunoblotting shows changes in γ -H2AX after radiotherapy in GSC 3028 (stiff) cells, with or without
116 IQGAP3.

117 **h**, Immunoblotting showed protein changes in GSCs (MES20 and 3028) and their corresponding DGCs
118 (MES20 and 3028) cultured on soft and stiff matrix gels after IR treatment.

119 **i - l**, GSCs (MES20 and 3028) cultured on stiff matrix gel, with or without IQGAP3 knockdown, were irradiated
120 with 2 Gy of IR. γ -H2AX foci at sequential time points post-irradiation were assessed using
121 immunofluorescence (**i** and **k**) and statistically quantified (**j** and **l**, n = 100 cells per group).

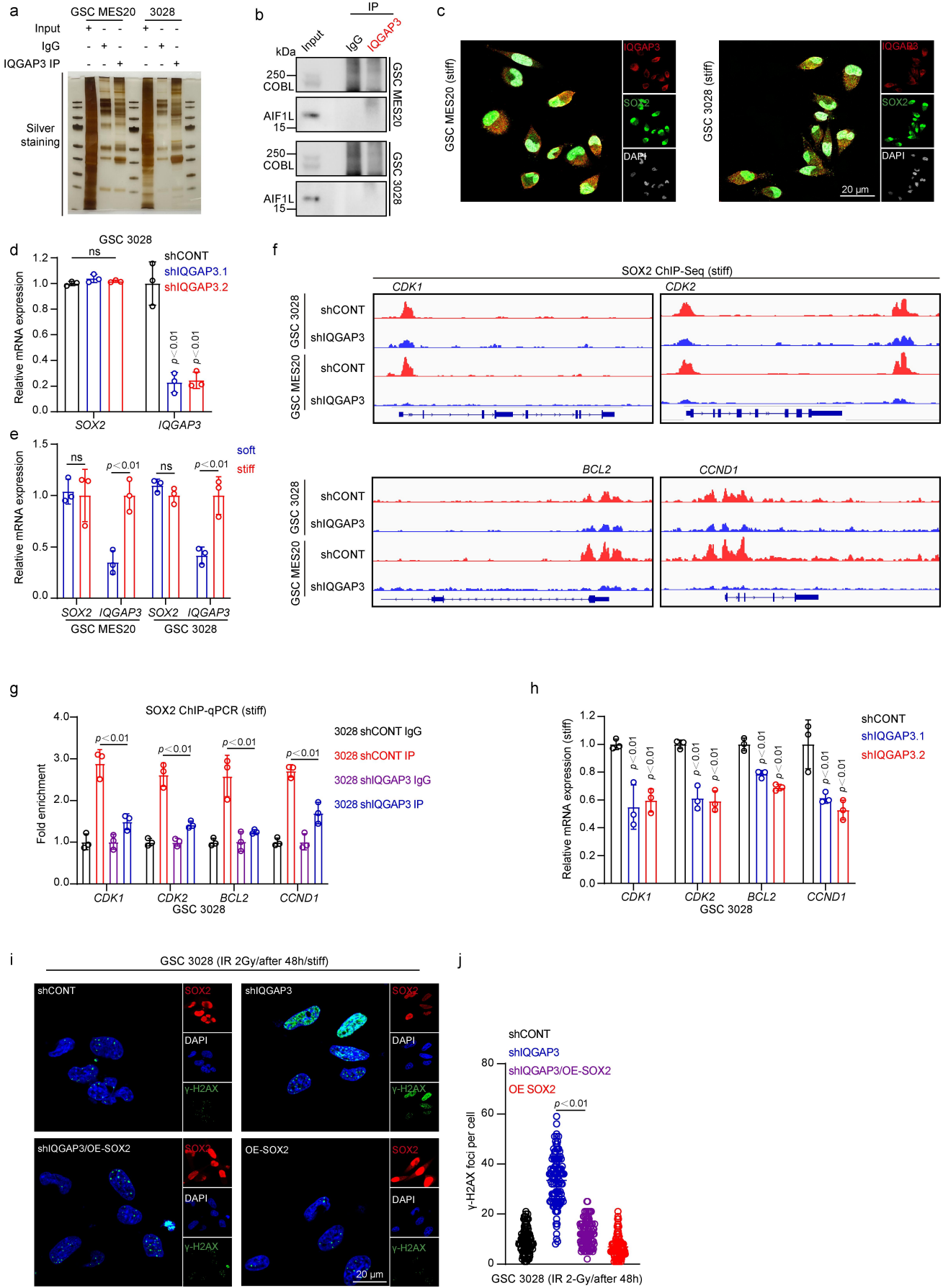
122 **m, n**, GSCs (3028), with or without IQGAP3 knockdown, were cultured on diffusion-based polyacrylamide
123 stiffness gradient gels and subjected to radiotherapy. Immunofluorescence experiments (**m**) and statistical
124 quantification (**n**) were performed 48 hours post-treatment to assess γ -H2AX fluorescence intensity. (n = 100
125 cells per group).

126 **o**, GSCs (3028), with or without IQGAP3 knockdown, were cultured on soft or stiff matrix gels and subjected
127 to radiotherapy, followed by quantification of cell proliferation. (n = 4)

128 **p**, Immunofluorescence staining shows that GSCs (3028), with or without IQGAP3 overexpression (OE), were
129 cultured on soft matrix gel and treated with IR.

130 In **b, d, f, j, l, n** and **o**, data are presented as mean \pm s.d. In **g** and **h** immunoblots are representative of three

131 independent experiments with similar results. In **b, d, f, j, l** and **n** data are presented from three independent
132 experiments. One-way ANOVA followed by multiple comparisons for **d**. Two-way ANOVA followed by multiple
133 comparisons for **b, f, j, l, n** and **o**. shIQGAP3: shIQGAP3.1 and shIQGAP3.2. IR: Ionizing Radiation (X-ray). ns,
134 not significant.



135 **Supplementary Fig. 9**

136 **a**, IP was performed for IQGAP3 protein in GSCs (MES20 and 3028) cultured on stiff matrix gel, followed by
137 analysis using immunoblotting and silver staining.

138 **b**, Immunoblot of IQGAP3 protein immunoprecipitates in GSCs (MES20 and 3028) cultured on stiff matrix gel.

139 **c**, GSCs (MES20 and 3028) were cultured on stiff matrix gel and subjected to immunofluorescence staining.

140 **d**, RT-qPCR analysis of GSCs (3028) cultured on stiff matrix gel with or without IQGAP3 knockdown.

141 **e**, RT-qPCR analysis was performed on GSCs (MES20 and 3028) cultured on soft and stiff matrix gels.

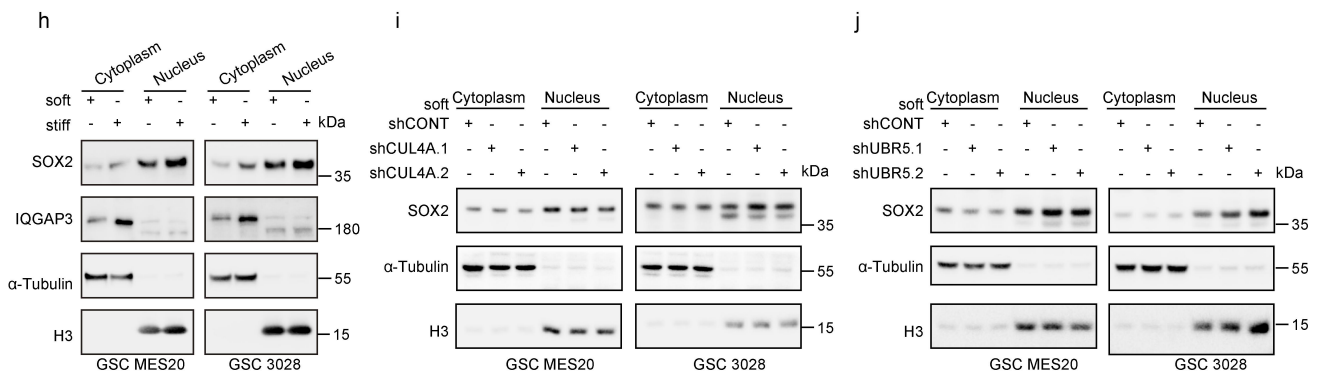
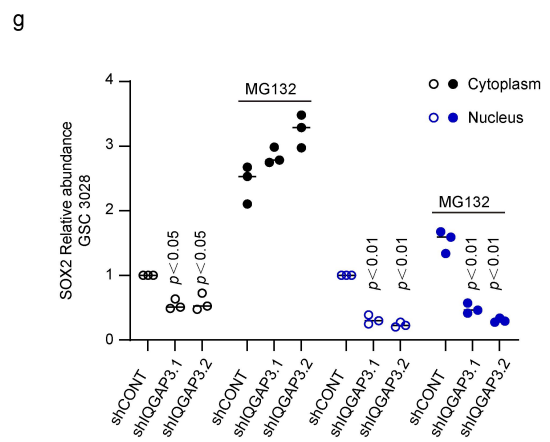
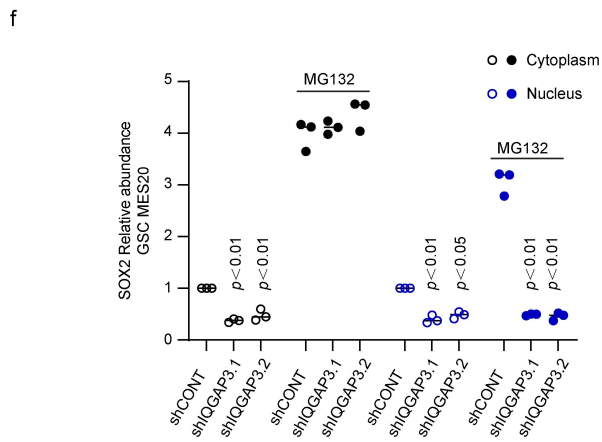
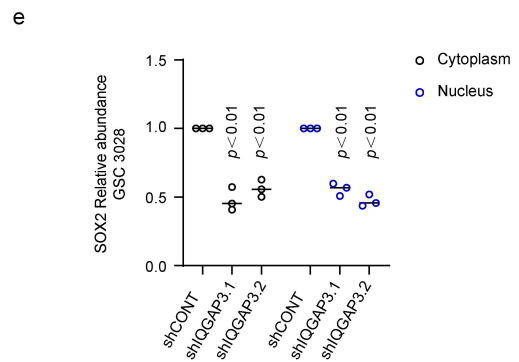
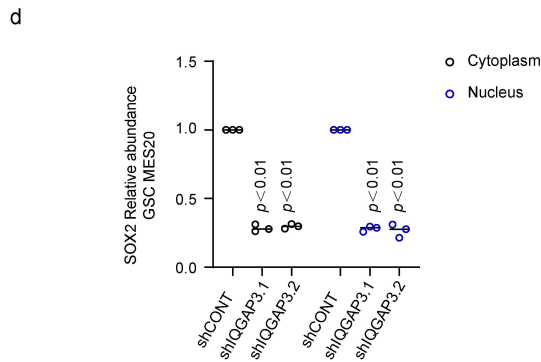
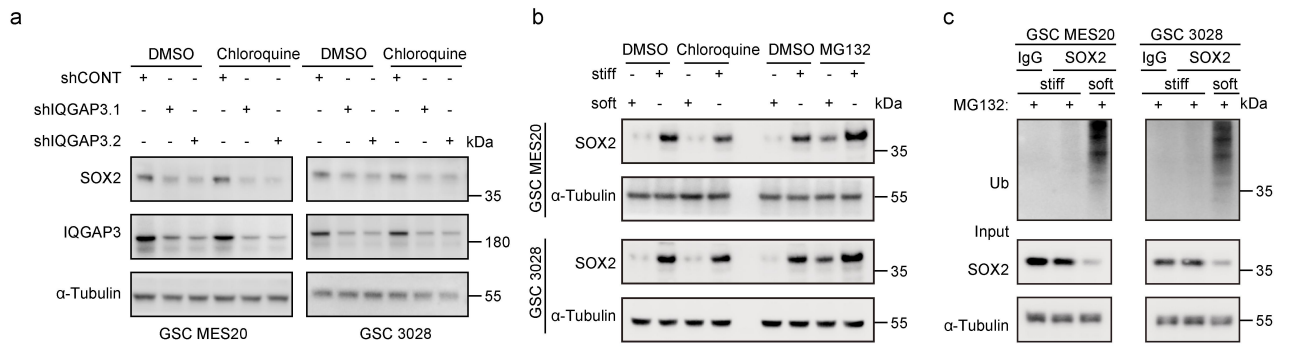
142 **f**, SOX2 ChIP-seq tracks at CDK1, CDK2, BCL2 and CCND1 gene loci.

143 **g**, SOX2 ChIP-qPCR analysis in GSC 3028 cultured on stiff matrix gel, with or without IQGAP3 knockdown.

144 **h**, RT-qPCR analysis of GSC 3028 cultured on stiff matrix gel with or without IQGAP3 knockdown.

145 **i, j**, GSCs (3028) were cultured on a stiff matrix gel, with or without IQGAP3 knockdown, followed by SOX2
146 overexpression after IQGAP3 knockdown. Following IR treatment, immunofluorescence (**i**) and quantification
147 (**j**) were performed 48 hours later (n = 100 cells per group).

148 In **d, e, g, h** and **j**, data are presented as mean \pm s.d. In **b**, immunoblots are representative of three
149 independent experiments with similar results. In **d, e, g, h** and **j**, data are presented from three independent
150 experiments. One-way ANOVA followed by multiple comparisons for **j**. Two-way ANOVA followed by multiple
151 comparisons for **d, e, g** and **h**. IP: immunoprecipitation. shIQGAP3: shIQGAP3.1 and shIQGAP3.2. IR: Ionizing
152 Radiation (X-ray). ns: not significant.



153 **Supplementary Fig. 10**

154 **a**, Immunoblot of GSCs (MES20 and 3028) cultured on a stiff matrix gel, with or without IQGAP3 knockdown,
155 after treatment with chloroquine to inhibit lysosomal degradation.

156 **b**, Immunoblot of GSCs (MES20 and 3028) cultured on matrigel with different stiffness, treated with
157 chloroquine and MG132 to inhibit lysosomal and proteasomal degradation, respectively.

158 **c**, Immunoblot of SOX2 ubiquitination levels in GSCs (MES20 and 3028) cultured on Matrigel with different
159 stiffness.

160 **d, e**, Immunoblot quantification of nuclear and cytoplasmic SOX2 fractions in stiff matrix gel-cultured MES20
161 and 3028 GSCs with/without IQGAP3 knockdown.

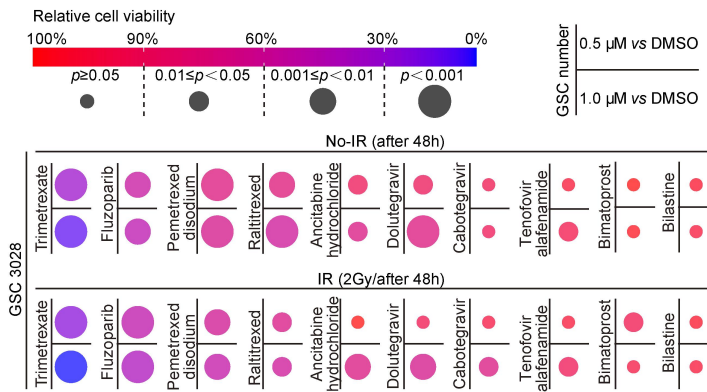
162 **f, g**, Immunoblot quantification of nuclear and cytoplasmic SOX2 fractions in stiff matrix gel-cultured MES20
163 and 3028 GSCs with/without IQGAP3 knockdown following proteasomal inhibition by MG132.

164 **h**, Immunoblot of nuclear and cytoplasmic fractions of GSCs cultured on matrigel with different stiffness.

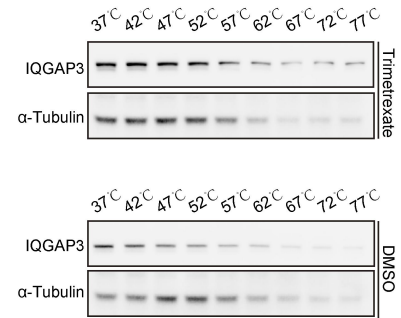
165 **i, j**, Immunoblot of nuclear and cytoplasmic fractions of GSCs (MES20 and 3028) cultured on a soft matrix gel
166 after knockdown of UBR5 (**e**) and CUL4A (**f**).

167 In **d - g**, data are presented as mean \pm s.d. In **a - c** and **h - j** immunoblots are representative of three
168 independent experiments with similar results. One-way ANOVA followed by multiple comparisons for **d - g**.

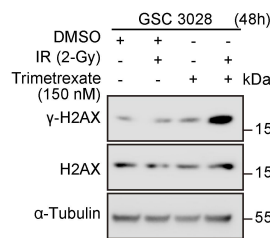
a



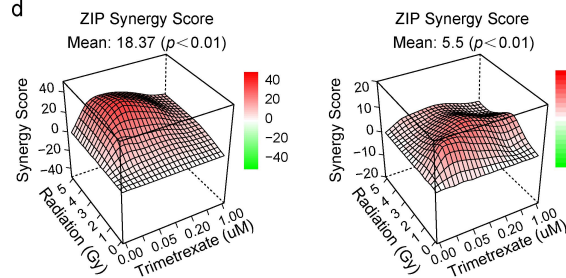
b



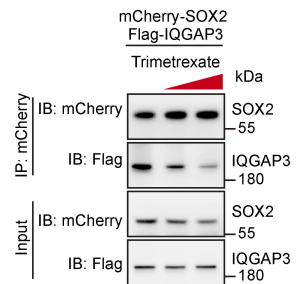
c



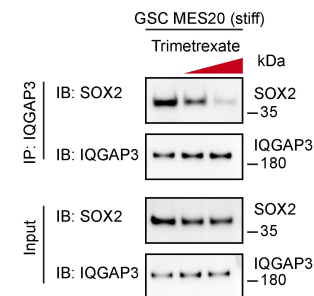
d



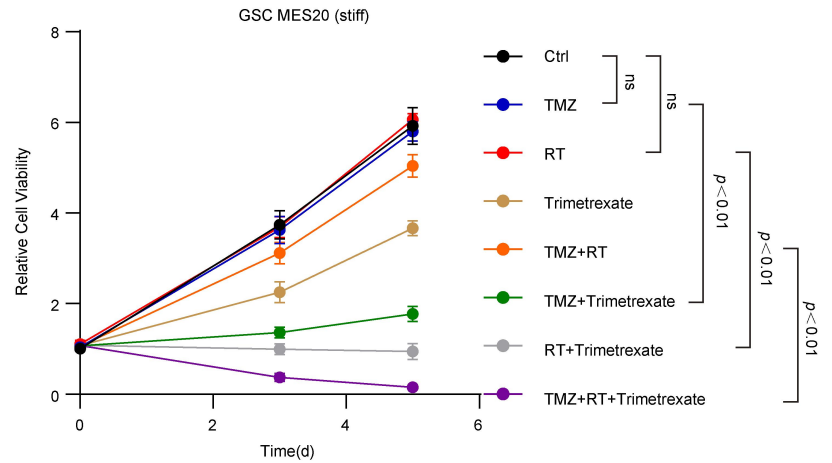
e



f



g



169 **Supplementary Fig. 11**

170 **a**, Effects of top 10 compounds on cell viability in GSC 3028 cells.

171 **b**, Immunoblot of IQGAP3 from CETSA in HEK293T cells overexpressing Flag-IQGAP3, pretreated with 200 nM
172 Trimetrexate.

173 **c**, Immunoblot of GSCs (MES20) cultured on a stiff matrix gel after treatment with IR or Trimetrexate.

174 **d**, 3D surface plot showing the effects of combined Trimetrexate and IR treatment on GSCs (MES20) cultured
175 on stiff (left) and soft (right) matrix gels after 48 hours.

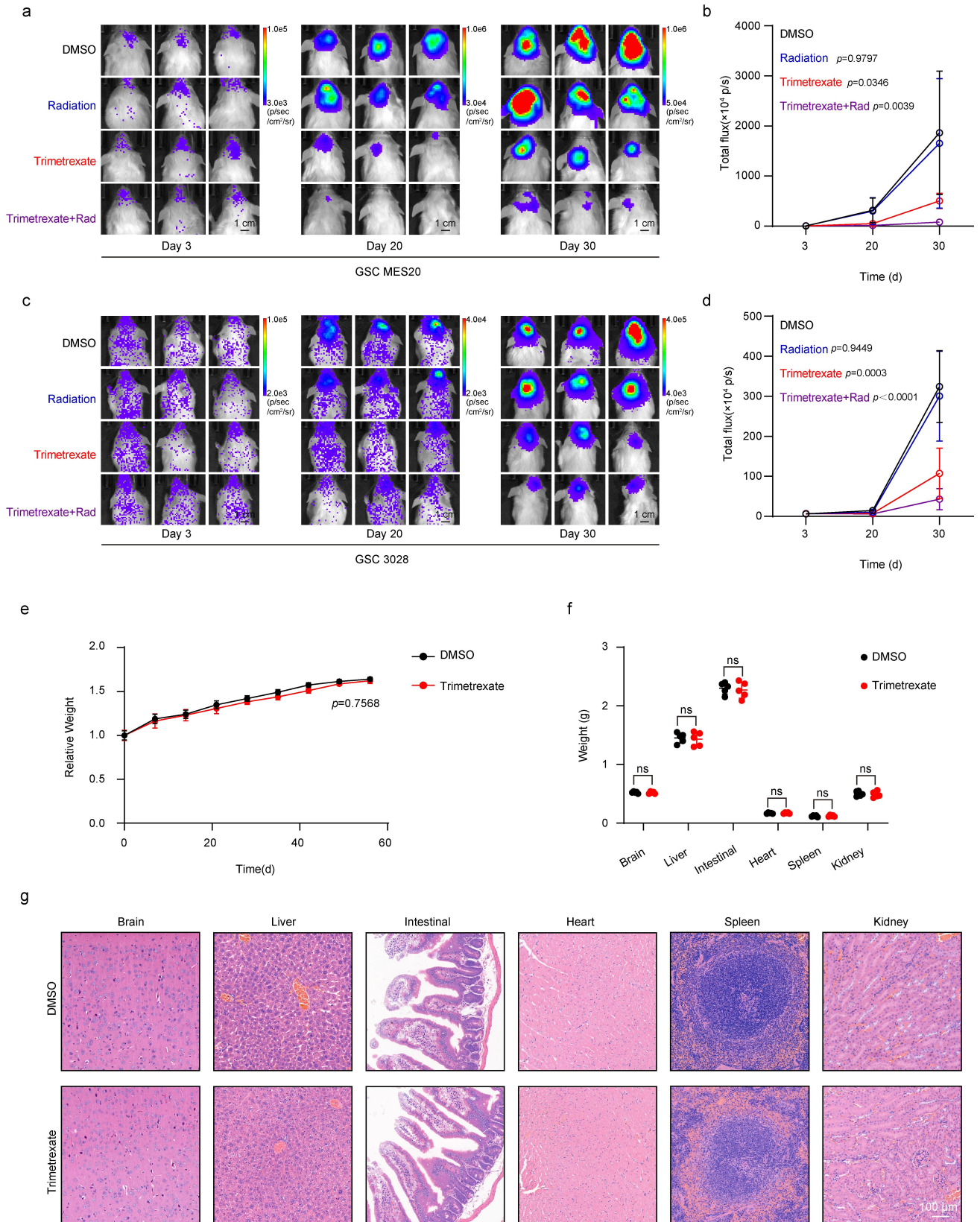
176 **e**, Immunoblot of mCherry-IP was performed on HEK293T cells overexpressing mCherry-SOX2 and
177 Flag-IQGAP3 after treatment with gradually increasing concentrations of Trimetrexate (0 nM, 100 nM, 200
178 nM) for 6 hours.

179 **f**, Immunoblot of IQGAP3-IP was performed on GSCs (MES20) after treatment with gradually increasing
180 concentrations of Trimetrexate (0 nM, 100 nM, 200 nM) for 6 hours.

181 **g**, Cell viability assay of GSCs (MES20) under different treatment conditions (n = 4).

182 In **g**, data are presented as mean \pm s.d. In **b**, **c**, **e** and **f**, immunoblots are representative of three independent
183 experiments with similar results. In **a** and **d**, data are presented from three independent experiments.

184 Two-tailed unpaired t-test for **a**. Two-way ANOVA followed by multiple comparisons for **g**. IP:
185 immunoprecipitation. IR: Ionizing Radiation (X-ray).



186 **Supplementary Fig. 12**

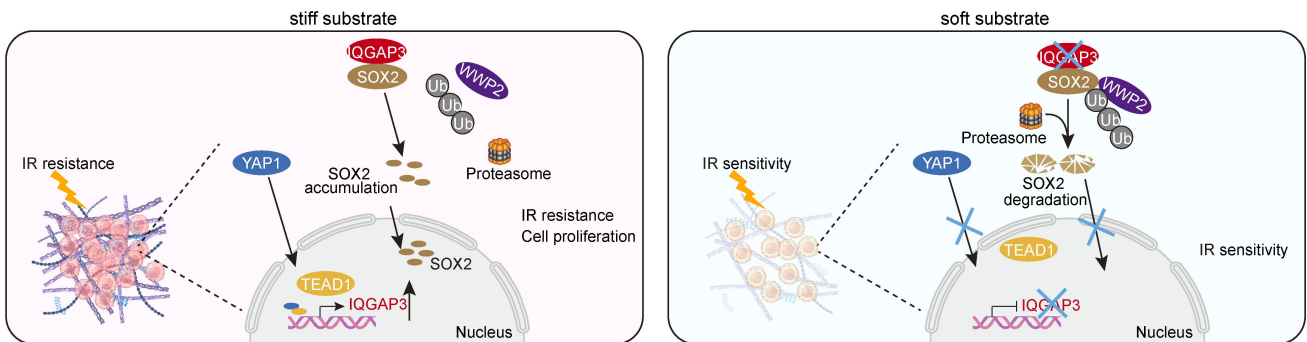
187 **a - d**, Representative in vivo bioluminescence imaging at the specified time point (**a** and **c**) and tumor growth
188 curves from in vivo bioluminescence analysis of mice carrying the indicated xenografts (**b** and **d**, n = 5 mice
189 per group).

190 **e**, Body weight change trend in mice receiving 5 consecutive days of intraperitoneal DMSO or trimetrexate
191 (10 mg/kg) injection.

192 **f**, Organ weight in mice receiving 5 consecutive days of intraperitoneal DMSO or trimetrexate (10 mg/kg)
193 injection.

194 **g**, Hematoxylin-eosin (HE) staining of mouse organs after 5 consecutive days of intraperitoneal DMSO or
195 trimetrexate (10 mg/kg) injection.

196 In **b, d, e** and **f**, data are presented as mean \pm s.d. Two-way ANOVA followed by multiple comparisons for **b, d**
197 and **f**. Two-tailed unpaired t-test for **e**. ns, not significant.



198 **Supplementary Fig. 13. Graphic abstract.**

199 Mechanical stimulation in stiff matrix induced expression of IQGAP3 in GSCs, leading to stabilization of SOX2
200 in the cytoplasm, and increased SOX2-mediated transcription of stemness and treatment resistance-related
201 pathways in the nucleus